Optimal Parameters and Characteristics of a Three Degree of Freedom Dynamic Vibration Absorber

Mariano Febbo
Instituto de Física del Sur (IFISUR) and CONICET
Departmento de Física,
Universidad Nacional del Sur,
Bahía Blanca 8000, Argentina
e-mail: mfebbo@uns.edu.ar

The present study is devoted to the determination of the optimal parameters and characteristics of a three degree of freedom dynamic vibration absorber (3 DOF DVA) for the vibration reduction of a plate at a given point. The optimization scheme uses simulated annealing and constrained simulated annealing, which is capable of optimizing systems with a set of constraints. Comparisons between a 3 DOF DVA and multiple (5) 1 DOF DVAs show a better performance of the former for vibration reduction. Regarding the characteristics of the optimal 3 DOF DVA, numerical tests reveal that the absorber is robust under variations of the observation point and for 10% variations of its mass, stiffness and damping. From the analysis of parameter changes of the plate, it is found that the optimal 3 DOF DVA is almost insensitive to a mass change, and sensitive to a change of Young's modulus for low frequencies. In this case, a decrease in Young's modulus causes a decrease in its effectiveness, and an increase improves it. The study of the effect of the 3 DOF DVA location on its effectiveness reveals that the requirements of closeness of the absorber to an antinode of the bare primary structure and to the observation point improve its performance. Additionally, for a rotational mode of the 3-DOF DVA about some axis, the effectiveness of the absorber at a given frequency can be notably increased if it is located at a position of the primary system with an in-phase or out-of- phase motion of the attachment points according to the rotational-mode characteristics of the 3-DOF DVA at this frequency. [DOI: 10.1115/1.4004667]

1 Introduction

To control undesirable high amplitudes of vibration of structural elements; for example plates, beams or rods, the addition of passive vibration-reduction mechanisms such as dynamic vibration absorbers (DVAs) constitutes an effective and robust solution. A DVA or, as referred to by some authors [1], tuned-mass damper (TMD), is composed of a discrete system, commonly a mass, a spring element and a damper, attached to the structure whose vibrations are to be reduced. This device was first proposed by Frahm in 1909 [2], and since then it has been continuously used for vibration control. The idea is simple: it consists in using a subsidiary system, the DVA, to reduce the vibration levels of the selected structure (primary system). Then, the vibration amplitude of the primary system is reduced by an increase in the displacement amplitude in the subsidiary system, which can dissipate some of the energy by the damper. The only requirement to gain a considerable reduction of the vibration level is that the natural frequency of the DVA has to be equal or close to the natural frequency of the main system. The effectiveness of the device is thus guaranteed, but in turn two unwanted effects appear: (1) the absorber is capable of controlling only one frequency of the main structure, and (2) its performance is extremely sensitive to the tuning between the natural frequency of the DVA and the resonant frequency of the main system. To avoid this difficulty, several techniques have been proposed to optimize the parameters of the DVA to minimize the response of the main system not only in the resonant frequency, but also in a range of frequencies near it. The seminal work of Ormondroyd and Den Hartog [3] was the foundation upon which many studies on vibration absorbers have been done. The model they developed constitutes an efficient method to perform this "broadband" vibration control. It relies on the existence of "invariant points" (points where the response of the whole system is independent of the amount of damping in the DVA) that appear only when the main system has no damping. Then, it is possible to find an optimum value for the stiffness and damping constants of the DVA by a parameterization of the response [4]. However, real systems always have some damping. Consequently, there exists a necessity to design new criteria to optimize real systems for vibration reduction.

This was the focus of a number of contributions on vibration absorbers over the last 30 years. Worthy of mention are the works of Jacquot [5], Thompson [6] and Kitis [7] among others, which proposed several ways to optimize single degree-of-freedom (SDOF) systems attached to beams or multiple-degree-of-freedom (MDOF) systems. More recently, some authors [8,9,10], have addressed the same problem by extending previous ideas to more general systems. Due to the possibility of controlling more than one mode, MDOF DVAs have been proposed over this and previous decades. Xu and Igusa [11] and Yamaguchi and Harnpornchai [12] used multiple DVAs to control the vibration amplitude of a SDOF primary system. Rice [13] showed the design of multiple discrete vibration absorber systems for broadband applications in structures modeled using modal data from finite element analysis. Zuo and Nayfeh [14] proposed an efficient numerical approach to maximize the minimal damping of modes in a prescribed frequency range for a general viscous or hysteretic MDOF tuned-mass systems, and more recently they optimized the stiffness and damping parameters for multiple tuned-mass dampers (MTDs) by decentralized control for parallel [15,16], and series [1] systems. On the same lines, Li and Ni [17] optimized nonuniformly distributed MTDs for vibration control, and, using simulated annealing, an optimal (parallel) two (2) DOF DVA was optimized by Febbo and Vera [18] to reduce the vibration levels of a beam over its first two resonances.

The aim of the present work is to numerically determine the optimal parameters and characteristics of a three (3) DOF DVA for the reduction of the vibration amplitude of a rectangular plate at a

Contributed by the Technical Committee on Vibration and Sound of ASME for publication in the JOURNAL OF VIBRATION AND ACOUSTICS. Manuscript received April 5, 2010; final manuscript received April 13, 2011; published online January 18, 2012. Assoc. Editor: Thomas J. Royston.

given point. The motivation to study a system with rotational as well as translational DOFs is based on the initial assumption that rotational DOFs would be very effective to reduce vibrations at positions of significant bending of the main system (plate). The solution is obtained using the simulated annealing technique and a constrained version of it, which permits a better adjustment of the results to the optimization requirements. In order to compare the effectiveness of the optimal 3 DOF DVA with simpler devices, the optimization of multiple (5) 1 DOF DVAs is also presented. Numerical tests on the robustness and effectiveness of the solutions in response to a parameter change of the plate and absorber are also carried out. Finally, the last section is devoted to the study of the effect of the 3 DOF DVA location on its effectiveness. The paper concludes with a summary of the results.

2 Mathematical Formulation

First, a sketch of the derivation of the equations is given. From all the possible ways to derive them, Lagrangian formalism is used here because it permits to model the plate-type structure separately and then couple it together with the dynamics of the attached system using the Lagrange multipliers approach. Figure 1(*a*) presents the system under study which consists of a plate (primary or main system) and a 3 DOF system attached to it. The intervening parameters of the 3 DOF system, m_e, I_{ex} and I_{ey} are, respectively, the lumped mass and mass moment of inertia in a direction parallel to the x and y axes; k_1, k_2, k_3, k_4, and c_1, c_2, c_3, c_4 are the spring and damper constants and a_1, a_2, a_3, a_4 are the distances between the center of mass and the corners of the rigid mass of the 3 DOF system (see Fig. 1(*b*). The total kinetic and strain energies and the dissipation function of the whole system (plate +3 DOF system) are:

$$T = \frac{1}{2}\sum_{i,j}^{n,n'} m_{ij}\dot{c}_{ij}^2 + \frac{1}{2}m_e\left(\frac{\dot{z}_{m1}a_2}{a_1+a_2} + \frac{\dot{z}_{m2}(a_4a_1 - a_3a_2)}{(a_1+a_2)(a_3+a_4)} + \frac{\dot{z}_{m3}a_3}{a_3+a_4}\right)^2 + \frac{1}{2}I_{ey}\left(\frac{\dot{z}_{m2}-\dot{z}_{m1}}{a_1+a_2}\right)^2 + \frac{1}{2}I_{ex}\left(\frac{\dot{z}_{m3}-\dot{z}_{m2}}{a_3+a_4}\right)^2 \quad (1)$$

$$V = \frac{1}{2}\sum_{i,j}^{n,n'} m_{ij}\omega_{ij}^2 c_{ij}^2 + \frac{1}{2}k_1(z_{m1}-z_1)^2 + \frac{1}{2}k_2(z_{m2}-z_2)^2 + \frac{1}{2}k_3(z_{m3}-z_3)^2 + \frac{1}{2}k_4(z_{m4}-z_4)^2 \quad (2)$$

$$D = \frac{1}{2}\sum_{i,j}^{n,n'} d_{ij}\dot{c}_{ij}^2 + \frac{1}{2}c_1(z_{m1}-z_1)^2 + \frac{1}{2}c_2(z_{m2}-z_2)^2 + \frac{1}{2}c_3(z_{m3}-z_3)^2 + \frac{1}{2}c_4(z_{m4}-z_4)^2 \quad (3)$$

where the c_{ij}'s are the normal mode amplitudes, ω_{ij} are the eigenfrequencies of the primary system and the $m_{ij}'s$ are given by $\rho h\int_\Omega \phi_{ij}\phi_{mn}d\Omega = \delta_{ij}m_{ij}$ (δ_{ij} is Kronecker's δ, ρ is the plate's mass density and h its thickness, see Fig. 1(*a*)). The internal damping of the plate is assumed to be of viscous type with d_{ij} as the modal damping parameters. Additionally, the transverse displacement of the plate is represented by $w(x, y, t) = \Sigma_{i,j}^{n,n\prime} c_{ij}(t)\phi_{ij}(x,y)$, where $\phi_{ij}(x, y)$ are the normal mode shapes of the selected plate. The summation is carried out up to the n, n' normal mode where the first $N = n \times n'$ modes are considered in order of increasing frequencies. Five restriction functions f_l's have to be imposed for the system of equations to be complete and solvable. This can be expressed by:

$$f_l = \sum_{i,j}^{n,n'} c_{ij}(t)\phi_{ij}(x_l, y_l) - z_l(t) = 0, \quad l = 1, ..., 4; \qquad f_5 = z_{m4} - (z_{m1} + z_{m3} - z_{m2}) \quad (4)$$

where the first four equations represent the connection of the 3 DOF system to the plate at the points x_l, y_l, $l = 1, 2, 3, 4$ (see Fig. 1(*b*)) and the fifth accounts for the rigidity condition of the mass of the 3 DOF system (rigid solid). Then, the equations of motion can be obtained by Lagrange's equations:

$$\frac{d}{dt}\left(\frac{\partial T}{\partial \dot{s}_k}\right) + \frac{\partial D}{\partial \dot{s}_k} + \frac{\partial V}{\partial s_k} = Q_k + \sum_{l=1}^{5}\lambda_l\frac{\partial f_l}{\partial s_k} \quad k = 1, ...N+8 \quad (5)$$

where the Q_ks represent the generalized forces applied at the point (x_f, y_f) and the λ_ls are Lagrange's multipliers. Finally, Lagrange's equations of motion yield, after the elimination of the λ_l's, a set of $N+3$ coupled linear second-order differential equations in terms of the new independent set of coordinates $\mathbf{q} \equiv [q_1, \ldots q_N, q_{N+1}, q_{N+2}, q_{N+3}] \equiv [c_{11}, \ldots c_{nn}', z_{m1}, z_{m2}, z_{m3}]$, and the set of generalized forces $\mathbf{Q} \equiv [Q_1, \ldots Q_N, 0, 0, 0]$:

$$\mathbf{M}\ddot{\mathbf{q}}(t) + \mathbf{C}\dot{\mathbf{q}}(t) + \mathbf{K}\mathbf{q}(t) = \mathbf{Q} \quad (6)$$

Matrices $(N+3 \times N+3)$ **M, C** and **K** are given by:

$$\mathbf{M} = \begin{bmatrix} \mathbf{M}_p & \mathbf{0} \\ \mathbf{0}^T & \mathbf{M}_{3\mathrm{DOF}} \end{bmatrix}; \quad \mathbf{C} = \begin{bmatrix} \mathbf{C}_p + \mathbf{C}_{\mathrm{sub}} & \mathbf{C}_c \\ \mathbf{C}_c^T & \mathbf{C}_{3\mathrm{DOF}} \end{bmatrix}; \quad \mathbf{K} = \begin{bmatrix} \mathbf{K}_p + \mathbf{K}_{\mathrm{sub}} & \mathbf{K}_c \\ \mathbf{K}_c^T & \mathbf{K}_{3\mathrm{DOF}} \end{bmatrix};$$

where the $(N \times N)$ matrices $\mathbf{M}_p$, $\mathbf{C}_p$ and $\mathbf{K}_p$ are diagonal matrices whose elements are m_k, $2\xi_k m_k\omega_k$ ($\xi_k = d_k/2m_k\omega_k$) and $m_k\omega_k^2$ ($k = 1, 2, \ldots N$), respectively. The rest of the matrices, $\mathbf{K}_{\mathrm{sub}}$, $\mathbf{C}_{\mathrm{sub}}$, $\mathbf{K}_c$, $\mathbf{C}_c$ and $\mathbf{M}_{3\mathrm{DOF}}$, $\mathbf{C}_{3\mathrm{DOF}}$, $\mathbf{K}_{3\mathrm{DOF}}$ are given in Appendix A.

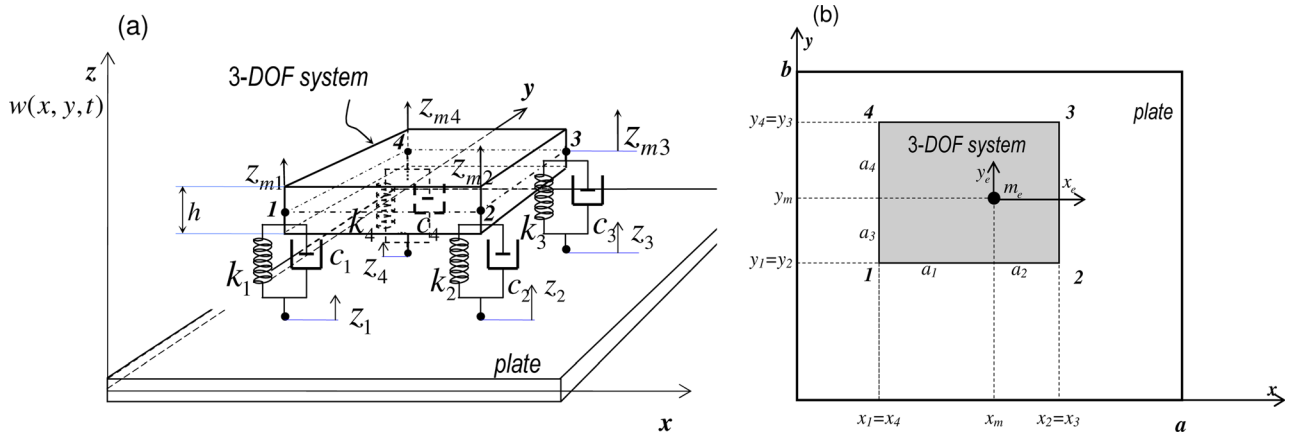

Fig. 1 (*a*) Plate with a 3 DOF system attached to it. (*b*) Nomenclature for the coordinates selected to describe the motion of the 3 DOF system

In order to calculate the displacement amplitude $\mathbf{q}(t)$ of the coupled system, a simple harmonic motion of vector $q(t) = \bar{q}e^{i\omega t}$ is imposed. Then, vector $\bar{q}$ is obtained by solving

$$\bar{\mathbf{q}} = [-\omega^2\mathbf{M} + i\omega\mathbf{C} + \mathbf{K}]^{-1}\tilde{\phi}(x_f, y_f) \tag{7}$$

where $\tilde{\phi}(x_f, y_f) = [\phi_1(x_f, y_f)...\phi_N(x_f, y_f)000]^T$ Finally, the displacement of the primary system at the point (x_a, y_a) is $w(x_a, y_a, t) = \sum_{k=1}^{N} \bar{q}_k e^{i\omega t}\phi_k(x_a, y_a)$.

In case v 1 DOF systems with parameters k_i, c_i, $i = 1...$v wish to be included in the dynamics of the primary system, only a slight modification of the above formulation is necessary. Then, matrices $\mathbf{M}_p$, $\mathbf{C}_p$, $\mathbf{K}_p$, $\mathbf{K}_{\text{sub}}$, $\mathbf{C}_{\text{sub}}$ remain the same while $\mathbf{K}_c$, $\mathbf{C}_c$ and $\mathbf{M}_{3\text{DOF}}$, $\mathbf{C}_{3\text{DOF}}$, $\mathbf{K}_{3\text{DOF}}$ need to be modified. Finally, the new matrices result: $\mathbf{M}_{3\text{DOF}} = diag(m_i)$; $\mathbf{C}_{3\text{DOF}} = diag(c_i)$; $\mathbf{K}_{3\text{DOF}} = diag(k_i)$ and

$$\mathbf{K}_c = [-k_1\phi(x_1, y_1) - k_2\phi(x_2, y_2)... - k_v\phi(x_v, y_v)];$$
$$\mathbf{C}_c = [-c_1\phi(x_1, y_1) - c_2\phi(x_2, y_2)... - c_v\phi(x_v, y_v)]$$

3 Optimization of the Dynamic Vibration Absorbers (DVAs)

The optimization of the MDOF systems acting as DVAs is carried out using suitable numerical schemes to solve this high nonlinear global optimization problem. Selecting as objective the minimization of the response of the primary system at its first three frequencies of resonance, two alternatives are presented: multiple (5) 1 DOF DVAs and one 3 DOF DVA, which allow for a meaningful comparison. The selection of five 1 DOF DVAs is made arbitrarily since it only intends to provide one possible comparison of the 3 DOF DVA with a simple and widely known system.

To find the parameters of MDOF DVAs is a complex task from a mathematical and numerical point of view. Den Hartog's pioneering strategy based on the existence of fixed points is one way to find k and c of a 1 DOF DVA attached to an undamped analogous system. This strategy is called optimal H_∞ control in the modern language of vibration control. In the case of a 3 DOF DVA, it is necessary to find the parameters that minimize an eight-dimensional objective function whose parameters are: (k_1, k_2, k_3, k_4, c_1, c_2, c_3, c_4). The difficulty then, increases considerably. Earlier studies [18] proposed to extend Den Hartog's ideas to optimize a 2 DOF DVA. In the same spirit, a reduction of half the number of variables was obtained and; consequently, of the time of calculation and complexity of the problem. In this work, two strategies are implemented for the optimization of a 3 DOF DVA. The first one applies Den Hartog's criterion by means of a simulated annealing technique, as reported in a previous work [18]. This optimization procedure is called simply SA optimization. The second one, which may serve as a test and an alternative for the first one, addresses directly the eight-dimensional problem by a constrained simulated annealing algorithm, and is called CSA optimization.

3.1 Simulated Annealing and Constrained Simulated Annealing. The method of simulated annealing (SA) was first proposed by Kirkpatrick et al. [19] based on a previous work by Metropolis et al. [20]. Numerical optimization for large scale optimization problems demonstrates that SA works efficiently for combinatorial optimization (the famous traveling salesman problem [21]) for instance. Other examples that show the versatility and efficiency of the same scheme are: the designing of complex electrical circuits to optimize the locations of several hundreds of them to avoid the interference of the connecting wires [22], or the optimization of the design of constrained composite sound absorbers [23] (continuous parameters optimization). A brief description of the method and its implementation for a 2 DOF DVA parameter optimization can be seen in a previous work of the author [18].

Constrained simulated annealing [24] (CSA) is based on simulated annealing that normally does probabilistic descents in the search space, with probabilities of acceptance governed by a temperature that is reduced in an exponentially decreasing fashion. Constrained simulated annealing, in contrast, increases the original search space $X \in \mathbb{R}^n$ by a Lagrange multiplier space $\Lambda \in \mathbb{R}^m$ and does probabilistic ascents in the Λ space and probabilistic descents in the original variable space. Then, if $f(\mathbf{x})$ is the objective function of the original problem, and there exists m equality constrains of the form $h_i(\mathbf{x}) = 0$, $i = 1...m$, the new increased objective function to be minimized is proposed to be: $L(\mathbf{x}, \lambda) = f(\mathbf{x}) + \Sigma_{i=1}^{m} \lambda_i |h_i(\mathbf{x})|$ which allows to obtain the optimal $\mathbf{x}_o$ subjected to the restrictions $h_i = 0$; $i = 1,..., m$. A flow diagram of the constrained simulated annealing scheme is shown in Fig. 2.

The procedure is extracted from Ref. [24] with some modifications introduced by the author in the trial point generation routine based on a previous work [18]. For the sake of brevity, the salient features of the algorithm are shown here. The algorithm starts generating a starting point $(\mathbf{x}, \lambda)$ which can be either user provided or randomly generated ($\lambda = \{\lambda_1, \lambda_2,..., \lambda_m\}$) is initialized to zero). Then, the temperature T (control parameter) is set to be high enough (to be discussed later) so as to accept almost all trail points $(\mathbf{x}', \lambda')$. After that, N_T, which is the number of iterations at each temperature required to equilibrate the system is established to be $N_T = \zeta(20n + m)$ where $\zeta = 10(n + m)$ (see Corana et al. [25]). The next step is to generate a random trial point $(\mathbf{x}', \lambda')$ in the neighborhood of $(\mathbf{x}, \lambda)$ in the search space $S = X \times \Lambda$ using the generation routine mentioned above. After computing ΔL, if $\Delta L \leq 0$ the new solution is accepted. Otherwise, the algorithm rejects it unless the probability transition $prob\Delta L \geq rd$ (0,1), being rd (0,1) a uniformly distributed random number in the interval (0,1). The function $prob\Delta L$ consists of two components, depending on whether $\mathbf{x}$ or λ is changed:

$$prob(\Delta L) = \left\{ \begin{array}{ll} \exp\left(\dfrac{-(L(\mathbf{x}', \lambda') - L(\mathbf{x}, \lambda))}{T}\right) & \text{if} \quad \mathbf{x} \to \mathbf{x}' \\ \exp\left(\dfrac{-(L(\mathbf{x}, \lambda) - L(\mathbf{x}', \lambda'))}{T}\right) & \text{if} \quad \lambda \to \lambda' \end{array} \right\}$$

Once the iterations per temperature N_T are completed, temperature T is decreased by its cooling rate and the procedure starts again with $N_T = 0$ for a decreased T. The CSA algorithm stops when the current temperature is low enough (e.g., $T < 10^{-6}$). Finally, the algorithm requires an adjustment of two intervening parameters (see Corana [25]): the initial temperature T_0 and the cooling rate t_e. The initial temperature is generated by first randomly generating 100 points of $\mathbf{x}$ and their corresponding neighboring points $\mathbf{x}'$ where each component $|x_i' - x_i| \leq 0.001$ and then setting $T = max_{x,x',i}\{|L(\mathbf{x}', 1) - L(\mathbf{x}, 1)|, |h_i(\mathbf{x})|\}$. The cooling rate is set to be 0.8 for all the numerical experiments.

4 Numerical Optimization Results

Appropriate numerical experiments for the determination of the optimal parameters of a 3 DOF DVA based on SA and CSA are presented. Five 1 DOF DVAs are also optimized (see Fig. 3) to compare their performances to the optimized 3 DOF DVA.

The optimization of a 1 DOF DVA attached to a primary system has been already discussed by several authors. Since it is not the aim of this work to propose a rule to optimize systems of this kind, a traditional optimization scheme is followed based on Den Hartog's optimization procedure. This particular optimization procedure has been implemented by Cheung [10], who extends Den Hartog's method and considers a plate as the primary system. As it can be deduced from his work, the following procedure takes into account neither the coupling between the DVAs nor the internal viscous damping in the plate. As a result, tuning ratio (α_a) and damping coefficient (ξ_{ma}) are given by:

$$\alpha_a = \frac{1}{1 + \mu\phi_{ij}^2(x_\nu, y_\nu)}$$

and

$$\xi_{ma} = \sqrt{\frac{3\mu\phi_{ij}^2(x_\nu, y_\nu)}{8(1 + \mu\phi_{ij}^2(x_\nu, y_\nu))^3}}$$

where $\phi_{ij}(x_\nu, y_\nu)$ is the modal shape function of the normal mode at the DVA location. The location of each DVA is schematically represented in Fig. 3 where the first DVA (1) is located at the center of mass of the 3 DOF DVA and the rest of them (2,3,4,5) are placed at the corners. With these locations, the first DVA (1) is selected to reduce the vibration amplitude for the first resonance of the plate, DVA (2) and DVA (4) are set to reduce the third and DVA (3) and DVA (5) are chosen for the second. Clearly, other combinations are also possible and it is possible to find which way is better for each different DVA location. However, it can be shown (numerically) that the final results are all comparable to each other.

The optimization of the 3-DOF DVA by SA proposed here is based on an extension of the method presented by the author [18] for a 2-DOF DVA. The approach uses Den Hartog's scheme for the optimization problem and; as a result, it presents a reduction of half the number of parameters to be optimized.

On the other side, the optimization by CSA solves the case of an eight-dimensional optimization problem. Accordingly, a conveniently selected objective function which depends on parameters $\mathbf{k} = (k_1, k_2, k_3, k_4)$ and $\mathbf{c} = (c_1, c_2, c_3, c_4)$ is proposed

$$f(\mathbf{k}, \mathbf{c}) = W_1(\mathbf{k}, \mathbf{c}) + W_2(\mathbf{k}, \mathbf{c}) + W_3(\mathbf{k}, \mathbf{c}) \tag{8}$$

where $W_p(\mathbf{k}, \mathbf{c}) = \sum_{i=1}^{s_1} |W(\mathbf{k}, \mathbf{c}, \omega = \omega_i,)|$ for $\omega_{pj} - \delta \leq \omega \leq \omega_{pj} + \delta, (j = 1, 2, 3)$. Here, ω_{pj} are the first three natural frequencies of the primary system and δ is a selected frequency interval (for example $\pm 0.1\ \omega_p$). This means that the objective function takes into account not only the displacement amplitude at the three resonances but also many frequency points near them. For all the cases, 10 points ($s_i = 10$) are selected in each summation. This is a compromise solution between calculation time and accuracy of the solution. However, there exists a problem with this objective function since no restriction on the stiffness constant values of the 3 DOF system (k_1, k_2, k_3, k_4) is required. It may then occur that the absorber has its natural frequencies far away from the first three resonances of the plate, resulting in a poor optimization. For this reason, three restrictions functions, h_1, h_2, h_3 are added to the objective function to consider this effect. The new objective function reads

$$f(\mathbf{k}, \mathbf{c}) = W_1(\mathbf{k}, \mathbf{c}) + W_2(\mathbf{k}, \mathbf{c}) + W_3(\mathbf{k}, \mathbf{c}) + \sum_{i=1}^{3} \lambda_i |\omega_i^{(3DOF)} \times (\mathbf{k}, \mathbf{c}) - \omega_{pi}| \tag{9}$$

where ω_{pi} is the *i-th* natural frequency of the plate (the first three) and $\omega_i^{(3DOF)}$ **(k, c)** is the *i-th* proposed natural frequency of the 3 DOF system calculated by the algorithm at each iteration.

4.1 Comparison Between an Optimal 3-DOF DVA and 5 Optimal 1-DOF DVAs. Numerical optimizations (SA and CSA) are presented for four different locations of the 3 DOF DVA on the plate. As stated above, the performances of multiple (5) 1 DOF DVAs positioned at the same locations as the 3 DOF DVA

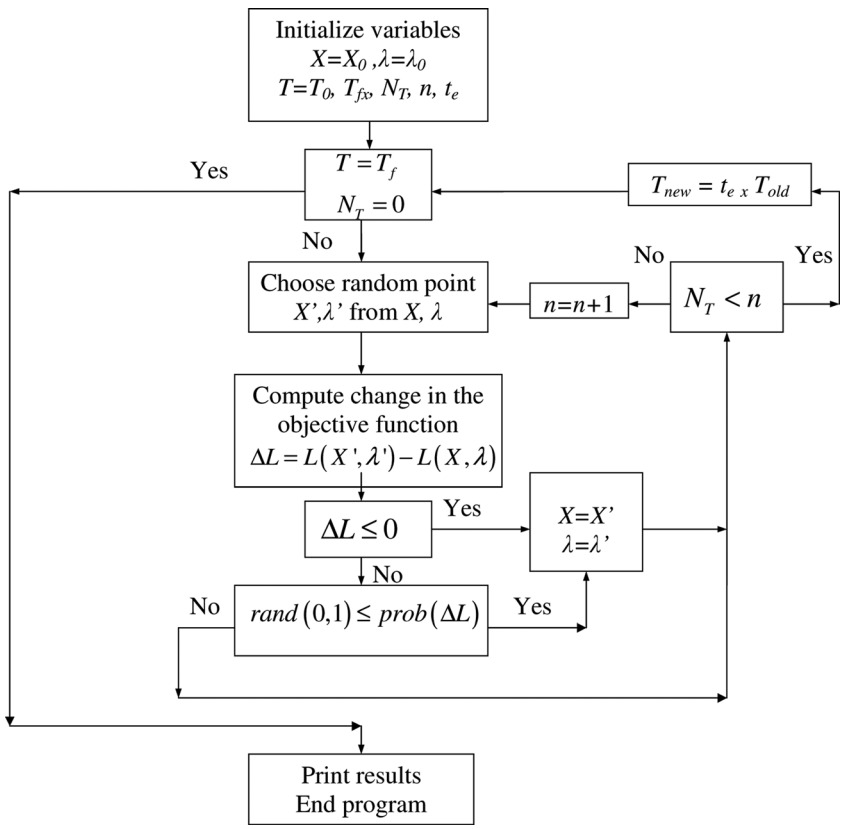

Fig. 2 Flow diagram for the implementation of the *constrained simulated annealing* algorithm CSA (see text for initial values of parameters)

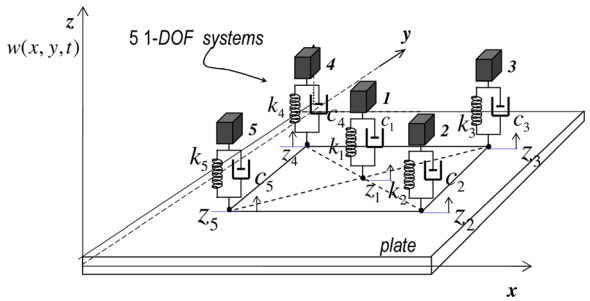

Fig. 3 Localization of five 1 DOF systems acting as DVAs for comparison with a 3 DOF DVA attached to the plate for vibration reduction

(with the disposition shown in Fig. 3) and with the same total mass as the 3 DOF DVA are also shown for comparison.

A totally simply supported steel plate of density 7.850×10^3 kg/m^3, length 2 m, Young modulus 2.051×10^1 1 N/m^2, height 0.005 m, width 1 m, mass 78.5 kg and damping coefficient 0.01 is considered for all cases. Thus, the first three natural frequencies of the undamped plate are: $f_1 = 15.19$ [Hz], $f_2 = 24.30$ [Hz] and $f_3 = 39.48$ [Hz]. The parameters of the 3 DOF DVA to be optimized are the stiffness and damper constants, i.e., k_1, k_2, k_3, k_4 and c_1, c_2, c_3, c_4. Its mass and mass moments of inertia remain the same for all the numerical experiments, as is usual in practice. They are chosen to be: $m_e = m_p/20 = 3.9250$kg, $h_e = 0.45$ m, $I_{ex} = (m_e/12)(h_e^2 + (a_3 + a_4)^2) = 0.0793\,\text{kgm}^2$, $I_{ey} = (m_e/12)(h_e^2 + (a_1 + a_2)^2) = 0.1688\,\text{kgm}^2$; $a_1 = a_2 = 0.28$ m; $a_3 = a_4 = 0.1$ m. Regarding this selection, it is necessary to clarify some points. In MDOF absorbers, both the mass of the absorber (as usually done in 1-DOF DVAs) and its geometric characteristics are usually specified for the optimization problem. In this case, this means to select: a_1, a_2, a_3, a_4, h_e, from which the mass moments of inertia I_{ex}, I_{ey} can be further obtained. Then, it is possible to ask which criterion must be adopted to propose such values. A reasonable criterion is to select a_1, a_2, a_3, a_4, h_e in order to make the natural frequencies of the 3-DOF DVA to be near the first three natural frequencies of the plate (this was previously adopted in Ref. [18]) and this is the one applied in this work. Certainly, there exist several ways to do this. However, and this is also according to the design philosophy of DVAs we only consider a 3-DOF DVA whose physical dimensions are comparably smaller than those of the plate and that also preserves the main characteristics of a 3-DOF system. In this process, considering the physical dimensions of the selected plate, the modes of the 3-DOF are predominantly rotation about the x axis (first mode), translation (second mode) and rotation about the y axis (third mode). Then, the optimization procedure has no possibility to change the mode's main characteristics and it can only modify the natural frequencies of the absorber (through k_1, k_2, k_3, k_4) and the damping constants). Naturally, other plate dimensions lead to the selection of a different 3-DOF absorber and to other optimization results for which the present method can perfectly be applied.

The observation point is selected at $(x_a, y_a) = (0.8125\text{m}, 0.3125\text{m})$ in order to obtain a nonvanishing displacement amplitude of the compound system. To determine its frequency response, the plate is excited by a sinusoidal source of variable frequency (0–50 [Hz]) located at $(x_f, y_f) = (0.3\text{m}, 0.3\text{m})$.

The four different locations of the 3 DOF DVA are schematically shown in Figs. 4(*a*), 4(*b*), and 4(*c*), together with the first three normal mode shapes of the bare plate. The location of the center of mass for the four cases are: (1) $(x_e, y_e) = (1.0, 0.5)$; (2) $(x_e, y_e) = (0.5, 0.5)$; (3) $(x_e, y_e) = (0.5, 0.75)$; (4) $(x_e, y_e) = (1.0, 0.75)$, which are selected in order to determinate how the effectiveness of the 3 DOF DVA changes under a variation of the type of motion of the plate (in-phase motion, out-of-phase motion) at the location of the absorber.

Before analyzing the results, it is appropriate to point out general aspects of MDOF systems attached to other (primary) systems. Firstly, if m-DOF systems ($m = 1, 2, 3,\ldots$) are attached to a primary system, the resulting (compound) system (plate + absorber) will have the sum of the degrees of freedom of the primary structure plus the m-DOFs provided by the added system. Then, if the MDOF systems have all their natural frequencies approximately tuned near the resonances of the primary system and their damping coefficients are not high, the new modes can be evidenced in a frequency response plot as additional peaks near the original resonances of the primary system.

These new normal modes, combined with those provided by the plate, will constitute the normal modes of the compound system and can be obtained, as well as the natural frequencies of the compound system, using Eq. (6), setting the RHS to zero. Figure 5(*a*) shows this case for our simply supported plate with an undamped ($c_1 = c_2 = c_3 = c_4 = 0$) 3-DOF system (solid line) with the same constants given above, and with k_1, k_2, k_3, k_4 given by the fourth row of Table 1 which ensures a proper tuning. When considering damping in the 3-DOF system, the previous situation changes in some way. It can be demonstrated that the presence of damping in the 3-DOF system gradually decreases the peak amplitudes, until they melt into a single peak of lower frequency than the original resonance when the damping is sufficiently high, in a similar fashion as it can be observed for heavily-damped 1-DOF absorbers. Figure 5(*a*) shows with a dashed dotted line the effect of a heavily-damped 3-DOF system ($c_1 = c_2 = c_3 = c_4 = 1000$) attached to a plate on the frequency response of the compound system. In brief, it can be said that, whereas the force exerted by the absorber in the plate is due to the springs in the undamped situation, in the extreme case of high damping the force is mainly due to the dampers.

With this in mind, it is easier to analyze the results of the optimization process for the four cases plotted in Figs. 1(*a*)–1(*d*). Numerical values of all the optimized parameters for cases [1–4] are presented in Table 1, as well as the normal-mode characteristics and natural frequencies of the 3-DOF system. Looking carefully at those figures, it is possible to conclude that the optimization results give a similar situation as the one explained above in the case of high damping of the 3-DOF: the existence of only one peak near each original resonance of lower amplitude and frequency serves as confirmation.

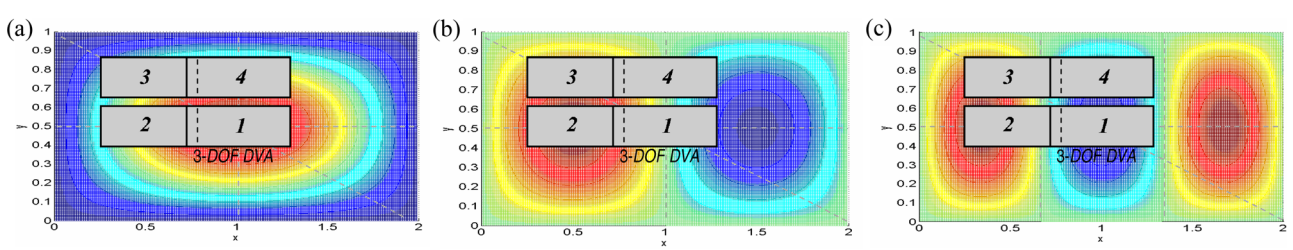

Fig. 4 First (*a*), second (*b*) and third (*c*) normal mode amplitudes of a totally simply supported (SSSS) rectangular plate; the four different selected locations [1–4] of the 3 DOF DVA mounted on the plate are also shown (see numerical values in text)

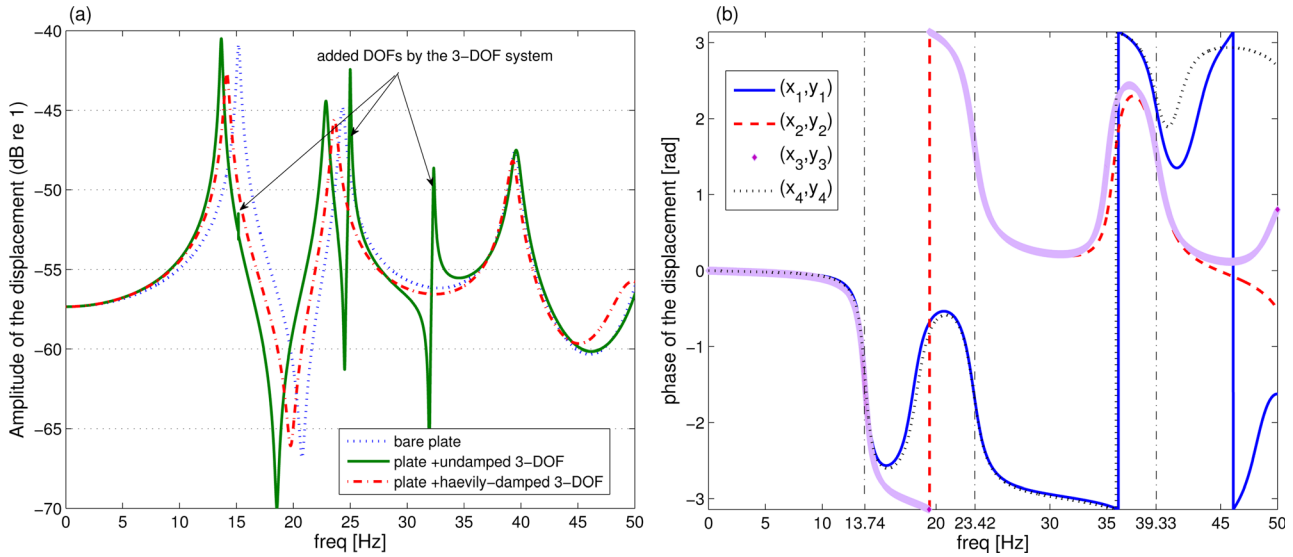

Fig. 5 (*a*) Amplitude of the displacement versus excitation frequency of a bare plate (dotted line), a plate with an undamped 3-DOF system attached to it (solid line), and a plate with a heavily-damped 3-DOF system attached to it (dashed dotted line). (*b*) Phase of the displacement of the compound system at the attachment points of the optimal 3 DOF DVA to the plate versus excitation frequency for case 1 (see text)

Concerning the performances of the optimization results shown in Figs. 6(*a*)–6(*d*), it can be said that both optimizations for the 3 DOF DVA (SA and CSA) give almost the same results for all cases. Specifically, for case 1 shown in Fig. 6(*a*), an important reduction of almost 5 dB for the first two resonances provided by the 3-DOF DVA is observed. At the third resonance, the reduction decreases slightly but it is still of 2.0 dB. On the other hand, the results of the five optimized 1 DOF DVAs (traditional optimization) reveal in principle a better reduction at the resonant frequencies of the bare plate. However, two undesirable peaks appear at both sides of those resonances. Therefore, they cannot be regarded as a better solution than that given by the 3 DOF DVA at this location. An exception must be made for frequencies near the third resonance where those peaks never exceed the amplitude that produces the optimized 3 DOF DVA and their performances are comparable.

For the second selected location of the DVAs (Fig. 6(*b*)), it is observed that the reduction provided by the 3-DOF DVA is not as good as that obtained in case 1 for the first resonance. On the contrary, for the second and third resonances, the reduction exceeds 5 dB and 4 dB, respectively. The optimization of the five 1 DOF DVAs gives a similar situation to that of Fig. 6(*a*): they present undesirable peaks at both sides of the resonances of the primary system, despite the fact that they notably reduced the amplitude for some frequency points in-between. Finally, the last two optimizations in Figs. 6(*c*) and 6(*d*) present similar characteristics to those obtained for the locations analyzed before. The results for the last selected location (Fig. 1 (*d*)) deserve some further comments. For the second and the third resonances, the reduction is very poor for the optimal 3 DOF DVA (less than 2 dB for the second, and 1.5 dB for the third).

From all this information, it is interesting to discuss the effect of the normal-modes characteristics of the 3-DOF system on the optimization results. Consider; for example, the poor performance of the absorber for case 1 at the third resonance (Fig. 1(*a*)). In order to explain this point, we plot in Fig. 5(*b*) the phase of the displacement of the compound system at the attachment points of the absorber to the plate as a function of excitation frequency. With dashed dotted lines we indicate the first three resonant frequencies of the compound system which are located at $f_1 = 13.74$[Hz], $f_2 = 23.42$[Hz] and $f_3 = 39.33$[Hz], respectively. For f_1 it can be observed that the 4 points have the same phase, clearly indicating an in- phase motion of the points. For the second maximum f_2, the points (x_1, y_1) and (x_4, y_4) on one hand and (x_2, y_2) and (x_3, y_3) on the other have the same phase, but both pairs of points are in an out-of-phase motion. Lastly, for the third maximum f_3, it is possible to observe that the phase of the four pairs of points is approximately the same, revealing an in-phase motion of all the points. Returning to our problem, the loss of effectiveness of the 3 DOF system at the third resonance in Fig. 6(*a*) can be attributed to the fact that the 3 DOF system is forced to make an in-phase motion at the points of attachment. Since this is not the predominant motion of its third mode, as it can be seen in Table 1, its effectiveness therefore notably decreases. Following a similar analysis, the other performances can be analyzed in the same way. We will return to this point in

Table 1 Results of the optimization of a 3 DOF DVA using SA and CSA methods for the four selected positions on the plate. The natural frequencies and predominant motion for each mode are also shown.

(x_e, y_e)	Method	k_1 [N/m]	k_2	k_3	k_4	c_1 [N seg/m]	c_2	c_3	c_4	mode 1 freq [Hz]	mode 2	mode 3
(1.0, 0.5)	SA	22630	15240	23624	13956	205.89	184.27	348.38	12.06	rot. x	transl.	rot. Y
	CSA	24786	14912	24857	14900	99.51	99.61	99.51	99.31	10.55	22.64	44.69
(0.5, 0.5)	SA	24235	17395	24264	16891	337.06	221.27	102.47	194.32	rot. x	transl.	rot. y
	CSA	23933	14537	24129	14435	169.22	169.25	168.07	168.67	10.39	22.29	44.00
(0.5, 0.75)	SA	27882	15511	27783	16855	349.95	231.47	349.72	349.48	rot. x	transl.	rot. y
	CSA	24378	14553	24042	14670	169.23	169.610	170.22	169.63	10.43	22.38	44.17
(1.0, 0.75)	SA	25820	16636	25560	15974	239.62	209.44	1.51	22.252	rot. x	transl.	rot. y
	CSA	23734	14161	24009	14182	165.32	162.18	165.66	164.70	10.31	22.15	43.73

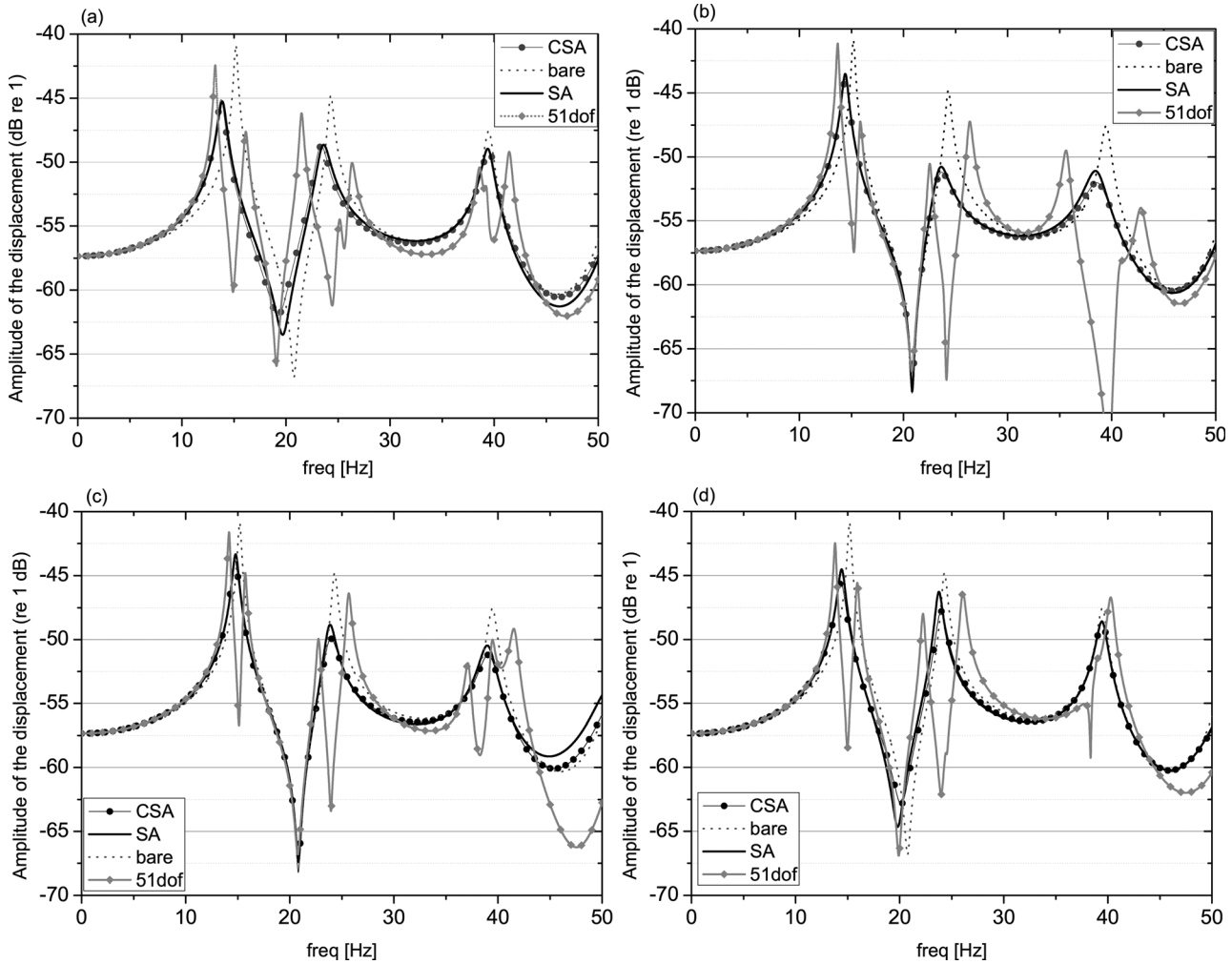

Fig. 6 (*a*) Amplitude of the displacement versus excitation frequency of a simply supported rectangular plate with five 1 DOF DVAs and one 3 DOF DVA. The five 1-DOF DVAs are located as shown in Fig. 4, and they change their positions in the same manner as the 3-DOF DVA. The center of mass of the 3 DOF DVA is located in (*a*): (x_e, y_e) = (1.0, 0.5); (*b*) (x_e, y_e) = (0.5, 0.5); (*c*) (x_e, y_e) = (0.5, 0.75) and (*d*) (x_e, y_e) = (1.0, 0.75). In the inset, "bare" indicates for the amplitude of the plate without attached systems.

Sec. 4.3, where the effect of the location on the effectiveness of the 3 DOF system is analyzed. Another feature of interest comes up when the absorber is located near a nodal line of some mode of the bare plate. In this case, the situation also results in a lack of effectiveness of the 3-DOF system (similar to that observed for the 1-DOF absorbers) exhibited for the second resonance of cases 1 and 4. Note also that case 4 has the poorest performance because it is located farther from the observation point than in case 1 (see Sec. 4.3 for discussion).

4.2 Study on the Effectiveness and Robustness of the Optimized 3 DOF DVA Under Parameter Change. A thorough study on the effectiveness and robustness of the optimal 3 DOF

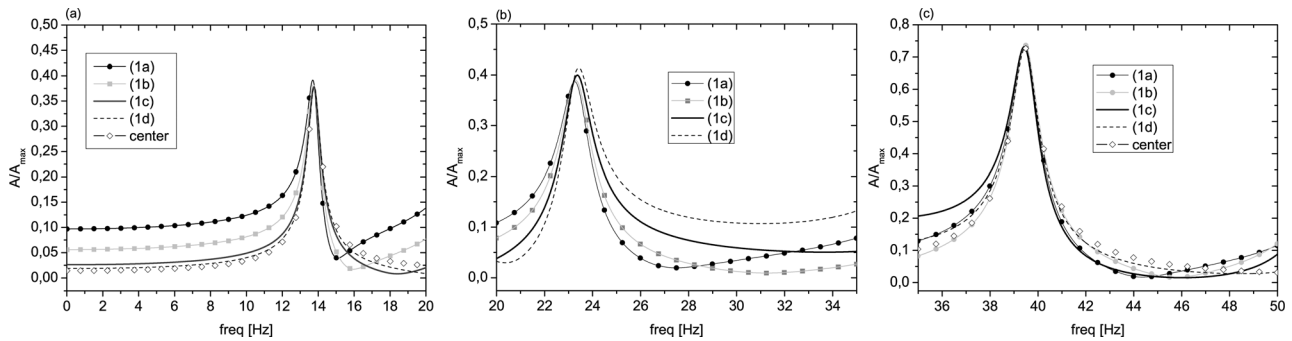

Fig. 7 Frequency response for a variation of the observation point for an optimal 3 DOF DVA attached to a SSSS rectangular plate. Frequencies near the first (*a*), second (*b*) and third (*c*) resonance of the plate. The curves are all normalized with respect to the amplitude at resonance (of the bare plate) for each frequency and observation point (see text for constants).

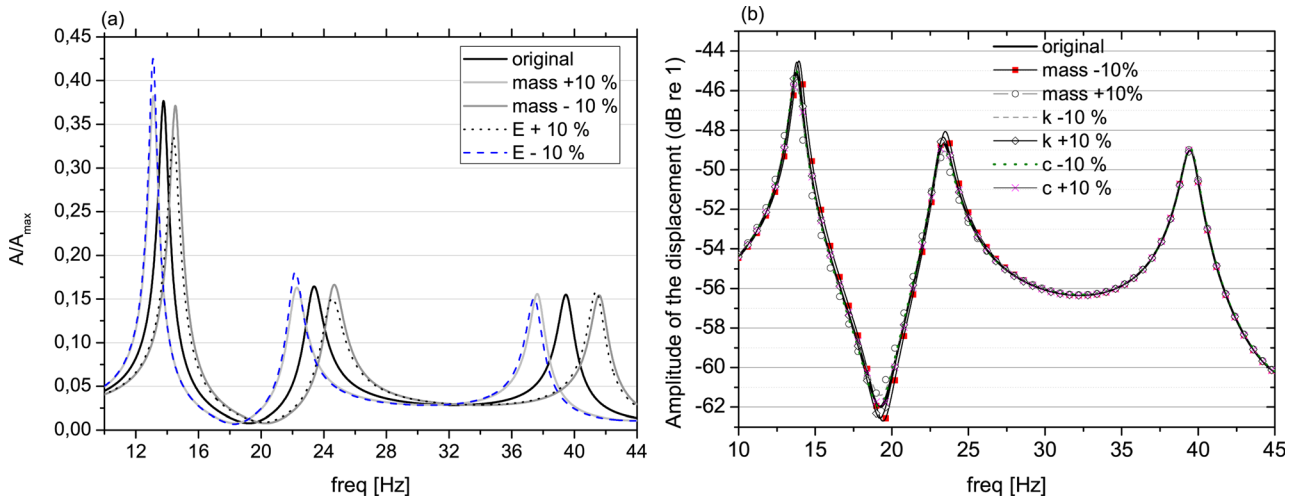

Fig. 8 (*a*) Robustness of the optimal 3 DOF DVA attached to a SSSS rectangular plate when the mass or Young's modulus (E) of the plate is decreased or increased by 10% compared with the original situation (original). The curves are all normalized with respect to the maximum amplitude of the first mode of the bare plate for each different case. (*b*) idem (*a*) for 10% variations of the mass, stiffness and damping constants of the optimal 3-DOF absorber.

DVA under some variations of the parameters of the plate and absorber is carried out in this section. The first variation to be analyzed is the change of the observation point. For this study, the absorber is located at the center of the plate. Since the optimal values of the 3 DOF DVA were calculated using $(x_a, y_a) = (0.8125, 0.3125)$, our intention is to see if a variation of the observation point produces a change on its effectiveness. For that purpose, several different points on the primary system are selected considering $(x_a, y_a) = (0.8125, 0.3125)$ as a reference point and leaving the other parameters of the 3 DOF DVA unchanged. Away from the center, positions (1a):$(x_a, y_a) = (0.25, 0.125)$, (1b):$(x_a, y_a) = (0.5, 0.25)$ and (1c):$(x_a, y_a) = (0.75, 0.375)$ are chosen in the main diagonal of the plate. Approaching the center, position (1d): $(x_a, y_a) = (0.875, 0.4375)$ and the center itself, $(x_a, y_a) = (1.0, 0.5)$, are selected. The observation points situated on the rest of plate (other quadrants) can be analyzed taking into account the symmetry of the mode under consideration. For example, if point $(x_{as}, y_{as}) = (1.1875, 0.6875)$ is observed (reflection with respect to the center taking $(x_a, y_a) = (0.8125, 0.3125)$ as the starting point) the displacement amplitude of the primary system results the same for frequencies near the first, second and third mode of the total system since these modes present symmetry with respect to that inversion. The results are shown in Figs. 7(*a*), 7(*b*), and 7(*c*). To provide a meaningful comparison, the frequency response curves are all normalized with respect to the amplitude at resonance (of the bare plate) for each frequency and observation point. It can be observed that the effectiveness of the 3 DOF DVA remains the same for the three figures. From an optimization viewpoint, it can be then concluded that the optimal system shows a robust performance for a variation in the observation point.

The results for a parameter change of the primary system are shown in Fig. 8(*a*), where the frequency response curves of the plate with the optimal 3 DOF DVA located at the center are depicted. For this variation variation, the mass or Young's modulus of the primary system is increased or decreased by 10%. The frequency response curves are all normalized with respect to the maximum amplitude of the first mode of the bare plate for each different case (mass + 10%, mass −10%, $E + 10\%$, $E - 10\%$). At first sight, it can be concluded that the behavior for the considered frequencies is different with the change of the maximum response peak. This effect is expected since the resonances of the primary system are changed in the same direction. Near the first and second resonances, the effectiveness of the 3 DOF DVA decreases when a reduction of 10% of Young's modulus is induced. With an increase in Young's modulus, the effectiveness of the 3 DOF DVA is improved for the first and second resonances. On the other hand, when the mass is increased or decreased by the same percentage, the effectiveness of the 3 DOF DVA is the same for the three resonances. At the third resonant frequency, there exists practically no change in the maximum peak reduction for the four variations.

Finally, the robustness of the 3 DOF DVA for 10% variation of its mass, stiffness and damping is analyzed. The results, shown in

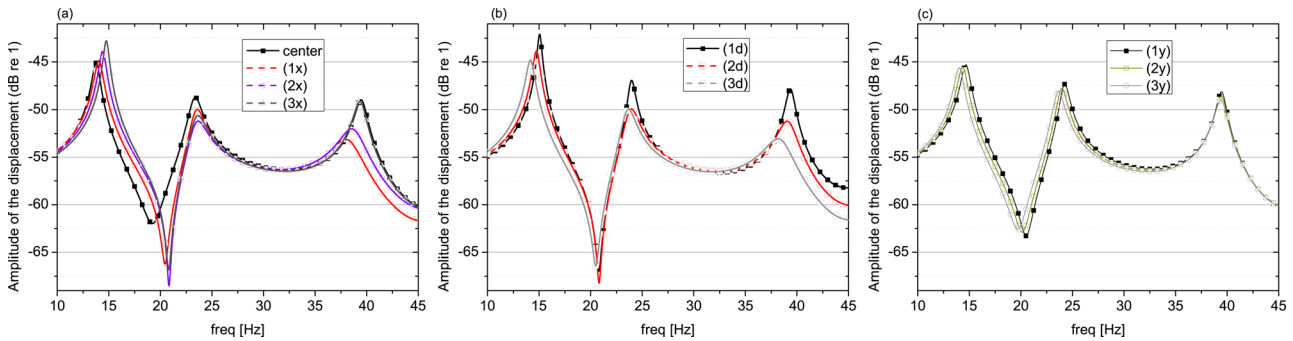

Fig. 9 Amplitude of the displacement versus excitation frequency of a SSSS rectangular plate with different optimal 3 DOF DVAs to compare their effectiveness under variations of their locations. The DVA is located in (*a*) three different positions on the middle line parallel to the *x* axis, (*b*) three different positions on the main diagonal and (*c*) other three different positions on the middle line parallel to the *y* axis (see text for numerical values).

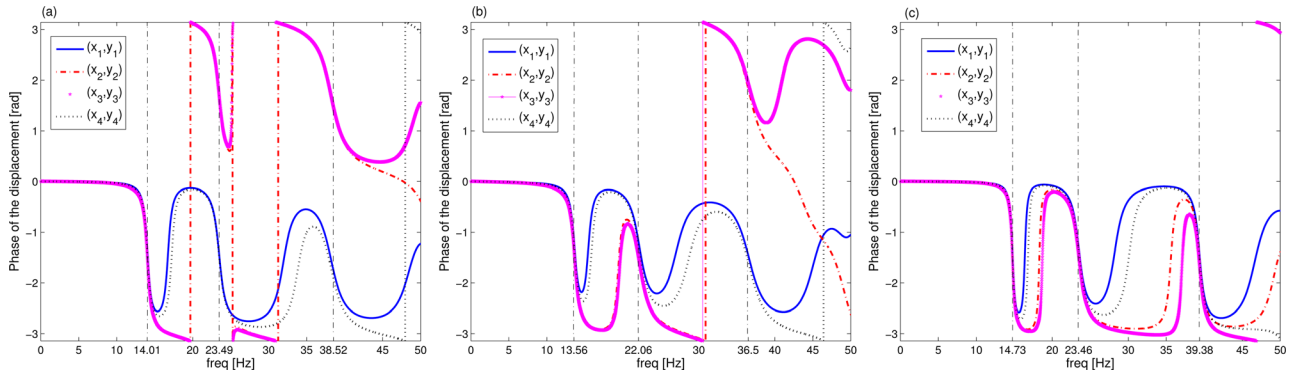

Fig. 10 Phase of the displacement of the compound system at the attachment points of the optimal 3 DOF DVA to the plate versus excitation frequency. The DVA is located in (*a*) 1*x*), in (*b*) 2*x*) and in (*c*) 3*x*) (see text). Dashed dotted lines indicates the resonant frequencies of the compound system in each case.

Fig. 8(*b*), suggest that the effectiveness of the 3 DOF DVA remains the same for all the variations regardless of the frequency under consideration. The major differences between the curves appear for the first resonance and never exceed 1 dB for the most dissimilar responses. Thus, it is possible to confirm that the optimal 3 DOF DVA is robust under the above variations.

4.3 Effect of the Location of the 3 DOF DVA on the Optimization Results. The theory [5] of single DOF DVAs mounted over continuum systems proposes that the effectiveness of a properly tuned absorber depends basically on two points. The first one is the closeness of the absorber to an antinode of the corresponding mode and the second one is the closeness of the point of attachment to the observation point. The aim of this section is to analyze whether additional requirements can be determined for a 3 DOF DVA having rotational DOFs. To this end, several cases are studied.

The cases under consideration are divided into three for DVAs located on the middle line parallel to the x axis (case 1), main diagonal (case 2) or the y axis (case 3). Figure 9(*a*) shows the frequency response curves for an optimal 3 DOF DVA located at three different positions on the middle line parallel to the x axis. These are (1x): $(x_e, y_e) = (0.75, 0.5)$, (2x): $(x_e, y_e) = (0.5, 0.5)$, (3x): $(x_e, y_e) = (0.3, 0.5)$. The results show that the best positions for vibration reduction at the first resonant frequency are the center of the plate and (1x). This is not the case for the second and third resonances. For the second resonance, the position labeled (2x) proves to be the best one, followed by (3x) and (1x), and for the third resonance, (1x) is notably better than the others. To understand these performances it is necessary to consider not only the two requirements for single DOF DVAs (explained in the first paragraph of this section), but also the phase of the displacement of the compound system at the attachment points of the absorber to the plate and the modes of the 3-DOF system. Firstly, it can be observed that the best locations for the first frequency fulfill both requirements of closeness (of the center of mass of the 3-DOF system) to the observation point and closeness to an antinode of the first mode of the plate. Additionally, the analysis of the phase of the displacement at the points of attachment for cases: center, Fig. 5(*a*), (1x), Fig. 10(*a*), (2x), Fig. 10(*b*), and (3x) Fig. 10(*c*), reveals that the motion of the compound system at the first frequency is an in-phase motion of all the points for all locations. Then, as it was previously discussed in Sec. 4.1, this prevents the rotational characteristics of the first mode of the 3 DOF system (rotation about the x axis) from having any influence, which results in a lack of effectiveness. The situation changes completely for the third resonant frequency, where an out-of-phase motion for cases 1x) and 2x) of points (x_1, y_1) and (x_2, y_2) (and (x_4, y_4) and (x_3, y_3)) increases significantly the effectiveness the 3 DOF system at these locations, since the third mode of the 3 DOF system is rotation about the y axis. This is not the case for the absorber located at the center of the plate and at location 3x, where an in-phase motion of all 4 attachment points decreases considerably the absorber's performance. For the second resonant frequency, the displacement amplitude of the bare plate has a nodal line passing through $x = 1$. Thus, a poor performance of the absorber located at the center is expected.

In Fig. 9(*b*) the DVA is located in several locations on the main diagonal of the plate. The locations are: (1d): $(x_e, y_e) = (0.3, 0.85)$, 2d): $(x_e, y_e) = (0.5, 0.75)$, 3d): $(x_e, y_e) = (0.75, 0.625)$. In this case, the best location occurs for position 3 d) which shows the best reduction for the three resonances. Again, this can be understood in terms of the above analysis.

Finally, Fig. 9(*c*) presents the frequency response for systems located at (1y): $(x_e, y_e) = (1, 0.85)$, (2y): $(x_e, y_e) = (1, 0.75)$, (3y): $(x_e, y_e) = (1, 0.625)$ (case 3). The noticeable feature in this case is that the three locations give similar results with a slightly better performance of (3y). This is due to the fact that (3y) is the location that fulfills the requirements of closeness both to an antinode (of the three normal modes of the bare plate) and to the observation point. The analysis of the phase of the displacement of the compound system at the points of attachment (not shown here for the sake of brevity) reveals that none of these three locations are in places whose phases are according to the rotational or translational characteristics of the modes of the 3-DOF DVA at the frequencies of interest. This means that; for example, for the third resonance, the absorber is located in a position with an in-phase motion of the attachment points for the three cases, preventing the 3-DOF system to rotate about the y axis, which corresponds to its third mode.

5 Conclusions

In the present work, an analytical and numerical procedure for the determination of the optimal parameters and characteristics of a 3 DOF DVA for the vibration reduction at a given point of a plate is carried out. The numerical optimization scheme uses simulated annealing (SA) and constrained simulated annealing (CSA), which is capable of optimizing systems with a set of equality constraints. These constraints are necessary if a suitable tuning of the natural frequencies of the absorber to the primary system is required, as in these cases. Numerical tests reveal that, for the cases studied, both methods, SA and CSA, give equal results. The comparison with multiple [5] optimal 1 DOF DVAs yields that the optimal 3 DOF DVA (CSA) presents a better solution for vibration reduction for the cases considered.

The variation of the observation point among five different possibilities shows that the 3 DOF DVA maintains its effectiveness for vibration reduction over the first three resonant frequencies. This means that the absorber can be optimized regardless of the observation point. From the analysis of parameter changes of the primary system, it results that the optimal 3 DOF DVA is almost

insensitive to a mass change, and it is sensitive to a change of Young's modulus for low frequencies (first two frequencies). In these cases, when Young's modulus decreases, the effectiveness is reduced, and when the opposite occurs, the effectiveness increases as well. Finally, numerical tests on the variation of the absorber's parameters reveal that the optimal 3 DOF DVA is robust for 10% variations in its stiffness, mass and damping.

The effect of location on the effectiveness of the 3 DOF DVA is thoroughly addressed. From the analysis of the results, it is possible to state that: (a) the requirements of closeness of the absorber to an antinode of the bare primary structure and closeness of the absorber to the observation point improve the effectiveness of the absorber; (b) for a rotational mode of the 3-DOF DVA about some axis, the effectiveness of the absorber at a given frequency can be considerably increased if it is located at a position of the primary system with an in-phase or out-of phase motion of the attachment points according to the rotational-mode characteristics of the 3-DOF DVA at this frequency.

5.1 A Mass, Damping and Stiffness Matrices. The $(N \times N)$ $\mathbf{C}_{\text{sub}}$ and $\mathbf{K}_{\text{sub}}$ matrices and the $(N \times 3)$ $\mathbf{C}_c$ and $\mathbf{K}_c$ rectangular matrices are:

$$\phi(x_l, y_l) = [\phi_1(x_l, y_l)\phi_2(x_l, y_l)...\phi_N(x_l, y_l)]^T$$

$$\mathbf{K}_{\text{sub}} = \sum_{l=1}^{4} k_1 \phi(x_l, y_l)\phi^T(x_l, y_l); \quad \mathbf{C}_{\text{sub}} = \sum_{l=1}^{4} c_1 \phi(x_l, y_l)\phi^T(x_l, y_l);$$

$$\mathbf{K}_c = [-k_1\phi(x_1, y_1) - k_4\phi(x_4, y_4) \quad -k_2\phi(x_2, y_2) + k_4\phi(x_4, y_4) \quad -k_3\phi(x_3, y_3) - k_4\phi(x_4, y_4)]$$

$$\mathbf{C}_c = [-c_1\phi(x_1, y_1) - c_4\phi(x_4, y_4) \quad -c_2\phi(x_2, y_2) + c_4\phi(x_4, y_4) \quad -c_3\phi(x_3, y_3) - c_4\phi(x_4, y_4)]$$

and the (3×3) symmetric matrices $\mathbf{M}_{3\text{DOF}}$ $\mathbf{C}_{3\text{DOF}}$ and $\mathbf{K}_{3\text{DOF}}$ are:

$$\mathbf{M}_{3\text{DOF}} = \begin{bmatrix} \frac{(m_e a_2^2 + I_{ey})}{(a_1 + a_2)^2} & \frac{m_e a_2(a_4 a_1 - a_3 a_2) - I_{ey}(a_3 + a_4)}{(a_1 + a_2)^2(a_3 + a_4)} & \frac{(m_e a_2 a_3)}{(a_1 + a_2)(a_3 + a_4)} \\ \frac{m_e a_2(a_4 a_1 - a_3 a_2) - I_{ey}(a_3 + a_4)}{(a_1 + a_2)^2(a_3 + a_4)} & \frac{m_e(a_4 a_1 - a_3 a_2) + I_{ey}(a_3 + a_4) + I_{ex}(a_1 + a_2)^2}{(a_1 + a_2)^2(a_3 + a_4)^2} & \frac{m_e a_3(a_4 a_1 - a_3 a_2) - I_{ex}(a_1 + a_2)}{(a_1 + a_2)(a_3 + a_4)^2} \\ \frac{(m_e a_2 a_3)}{(a_1 + a_2)(a_3 + a_4)} & \frac{m_e a_3(a_4 a_1 - a_3 a_2) - I_{ex}(a_1 + a_2)}{(a_1 + a_2)(a_3 + a_4)^2} & \frac{(m_e a_3^2 + I_{ex})}{(a_3 + a_4)^2} \end{bmatrix}$$

$$\mathbf{C}_{3\text{DOF}} = \begin{bmatrix} c_1 + c_4 & -c_4 & c_4 \\ -c_4 & c_2 + c_4 & -c_4 \\ c_4 & -c_4 & c_3 + c_4 \end{bmatrix};$$

$$\mathbf{K}_{3\text{DOF}} = \begin{bmatrix} k_1 + k_4 & -k_4 & k_4 \\ -k_4 & k_2 + k_4 & -k_4 \\ k_4 & -k_4 & k_3 + k_4 \end{bmatrix}$$

Acknowledgment

The present study has been sponsored by CONICET, and by Secretaría General de Ciencia y Tecnología of Universidad Nacional del Sur at the Departments of Physics (Grant No. PGI 24F/050).

References

[1] Zuo, L., 2009, "Effective and Robust Vibration Control Using Series Multiple Tuned-Mass Dampers," ASME J. Vibr. Acoust., **131**, p. 031003–1.

[2] Frahm, H., 1909, "Device for Damping Vibration Bodies," U. S. Patent No. 989958.

[3] Ormondroyd, J., and Den Hartog, J. P., 1928, "The Theory of the Vibration Absorber," J. Appl. Mech., **50**, pp. 9–22.

[4] Den Hartog, J. P., Mechanical Vibrations (McGraw-Hill, New York, 1956).

[5] R. G.Jacquot, 1978 "Optimal Dynamic Absorbers for General Beam Systems," J. Sound Vib., **60**, pp. 535–542.

[6] A. G.Thompson, 1981, "Optimum Tuning and Damping of a Dynamic Absorber Applied to a Force Excited and Damped Primary System, J. Sound Vib., **77**, pp. 403–415.

[7] Kitis, L., Wang, B. P., and Pilkey, W. D., 1983, "Vibration Reduction over a Frequency Range, J. Sound Vib., **89**, pp. 559–569.

[8] Ozer, M. B., and Royston, T. J., 2005, "Extending Den Hartog's Vibration Absorber Technique to Multi-Degree-of-Freedom Systems," ASME J. Vibr. Acoust., **127**, pp. 341–351.

[9] Asami, T., Nishihara, O., and Baz, A. M., 2002, "Analytical Solution to H_∞ and H_2 Optimization of Dynamic Vibration Absorber Attached to Damped Linear Systems," ASME J. Vibr. Acoust., **124**, pp. 67–68.

[10] Cheung, Y. L., and Wong, W. O., 2009, "H_∞ and H_2 Optimizations of a Dynamic Vibration Absorber for Suppressing Vibrations in Plates," J. Sound Vib., **320**, pp. 29–42.

[11] Xu, K., and Igusa, T., 1992, "Dynamic Characteristics of Multiple Substructures With Closely Spaced Frequencies," Earthquake Eng. Struct. Dyn., **21**, pp. 1059–1070.

[12] Yamaguchi, H., and Hampornchai, N., 1993, "Fundamental Characteristics of Multiple Tunned Mass Dampers for Suppressing Harmonically Forced Oscillations," Earthquake Eng. Struct. Dyn., **22**, pp. 51–62.

[13] Rice, H. J., 1993, "Design of Multiple Vibration Absorber Systems Using Modal Data," J. Sound Vib., **160**, pp. 378–385.

[14] Zuo, L., and Nayfeh, S. A., 2004, "Minimax Optimization of Multi-Degree-of-Freedom Tuned-Mass Dampers," J. Sound Vib., **272**, pp. 893–908.

[15] Zuo, L., and Nayfeh, S., 2005, "Optimization of the Individual Stiffness and Damping Parameters in Multiple Tuned-Mass Damper Systems," ASME J. Vibr. Acoust., **127**(1), pp. 77–83.

[16] Zuo, L., and Nayfeh, S. 2006, "The Two-Degree-of-Freedom Tunned-Mass Damper for Suppression of Single-Mode Vibration Under Random and Harmonic Excitation," ASME J. Vibr. Acoust., **128**, pp. 56–65.

[17] Li, H.-N, and Ni, X.-L., 2007, "Optimization of Non-Uniformly Distributed Multiple Tuned Mass Damper," J. Sound. Vib., **308**, pp. 89–97.

[18] Febbo, M., and Vera, S. A., 2008, "Optimization of a Two Degree of Freedom System Acting as a Dynamic Vibration Absorber," ASME J. Vibr. Acoust., **130** p. 011013.

[19] Kirkpatrick, S. Gelatt, C. D., and Vecchi, C. D., 1983, "Optimization by Simulated Annealing," Science, **220** (4598), pp. 671–680.

[20] Metropolis, N., Rosenbluth, A., Rosenbluth, M., Teller, A., and Teller, E., 1953, "Equation of State Calculations by Fast Computing Machines," J. Chem. Phys., **21**, pp. 1087–1092.

[21] Allwright, J. R. A. and Carpenter, D. B., 1989, "A Distributed Implementation of Simulated Annealing for the Travelling Salesman Problem," Parallel. Comput., **10**(3), pp. 335–338.
[22] M. P. Vecchi, and Kirkpatrick, S., 1983, "On the Optimal Location of Elementary Systems Using Simulated Annealing," IEEE Trans. Comput. Aided Des. **2**, pp. 215–222.
[23] Chang, Y., Yeh, L., and Chiu, M., 2005, "Optimization of Constrained Composite Absorbers Using Simulated Annealing," Appl. Acoust., **66**, pp. 341–352.
[24] Wah, B. W., Chen, Y. X., and Wang, T., 2007, "Simulated Annealing with Asymptotic Convergence for Nonlinear Constrained Global Optimization," J. Global Optim., **39**, pp. 1–37.
[25] Corana, A., Marchesi, M., Martini, C., and Ridella, S., 1987, "Minimizing Multimodal Functions of Continuous Variables with the Simulated Annealing Algorithm," ACM Trans. Math. Softw., **13**(3), pp. 262–280.
[26] Febbo, M., 2006, "Vibrations of Continuum Systems with Attached Discrete Elements: Dynamics and Optimization," Ph.D. thesis, Universidad Nacional del Sur, Bahía Blanca, Argentina (in Spanish).